Structure-Based Rational Design of β-Hairpin Peptides from Discontinuous Epitopes of Cluster of Differentiation 2 (CD2) Protein To Modulate Cell Adhesion Interaction

Jining Liu,[†] Cheng Li,[†] Shao Ke,[§,#] and Seetharama D. Satyanarayanajois*[,§]

Department of Pharmacy, National University of Singapore, 117543, Singapore, and Department of Basic Pharmaceutical Sciences, University of Louisiana Monroe, 700 University Avenue, Monroe, Louisiana 71209

Received January 22, 2007

Modulation or inhibition of interaction of cluster of differentiation (CD) adhesion molecules CD2−CD58 has been shown to be therapeutically useful. The analysis of the crystal structure of CD2 complexed with CD58 was carried out to define the epitopes that are important for the interaction of the two proteins. The crystal structure of CD2 indicated that the interaction surface of CD2 with CD58 has two β-strand structures (F and C strands) with charged residues. On the basis of the crystal structure of the complex CD2−CD58, we have designed β-hairpin peptides from the β-strand region of CD2 by conjugating the discontinuous sequences in the protein. The peptides were modeled by molecular dynamics simulation, and their inhibitory activities were evaluated in vitro using two heterotypic cell adhesion assays, E-rosetting and lymphocyte-epithelial cell adhesion assays. Results indicated that 12- and 14-residue conjugate cyclic peptides cKS12 and cDD14 exhibited 60% and 50% inhibition activity, respectively, at 90 μM.

Introduction

The cluster of differentiation (CD[a]) pair CD2−CD58 is an important adhesion molecular complex under investigation for immunological synapse formation between the T cell and the target cell.[1−4] Both CD2 and its ligand, leukocyte function associated antigen 3 belong to the immunoglobulin superfamily (IgSF).[5,6] The interaction between CD2 and CD58 is believed to augment the adhesion between the T cell receptor−major histocompatibility complexes (TCR−MHCs).[2] The adhesion between CD2 and CD58 causes a costimulatory signal in the T cell that amplifies the primary signal caused by the TCR−MHC. The affinity of the TCR−MHC is known to increase by 30- to 50-fold in the presence of CD2−CD58 interaction compared to the absence of the interaction. These findings make CD2 and CD58 molecules attractive targets to understand the mechanism of immunological synapse and autoimmune diseases.[7−9] The extracellular portion of the CD2 molecule can be divided into three regions via epitope mapping. Monoclonal antibodies directed against CD2 inhibited adhesion or modulated T cell activation, depending on the region of the epitope. In vitro studies suggested that anti-CD2 blocking antibodies inhibited T cell activation when added to mixed lymphocyte reaction. Inhibition of the CD2−CD58 interaction has important implications in controlling immune responses in autoimmune diseases.[10,11] Therefore, molecules designed to inhibit CD2−CD58 interaction may function as immunosuppressants. There are several reports of modulation of CD2−CD58 interactions for therapeutic use. The hybridoma cells producing mouse anti-rat CD2 mAb (OX34, IgG2a) treatment can prevent the induction of arthritis[12] and prolong graft survival, acting synergistically with cyclosporine.[13] BTI-322, formerly known LO-CD2a, a rat monoclonal IgG2bκ directed against the CD2 antigen on T cells and NK cells, blocks primary and memory alloantigen proliferative responses in vitro.[14] Studies showed that it is a safe and effective agent for prevention of rejection in renal allograft recipients,[15] kidney allograft rejection,[16] and acute graft versus host (GVH) disease. Blockade of CD2 was recently reported to be partially effective in severe psoriasis by using MEDI-507 (siplizumab), a humanized IgG1k anti-CD2 antibody.[17] Another biological agent, alefacept, directed against CD2 is a selective immunomodulating, antipsoriatic drug that blocks the CD2−CD58 interaction necessary for the activation and proliferation of memory effector T cells. It is a recombinant human CD58−Ig fusion protein, effectively binds to CD2, and prevents its interaction with CD58 expressed on APCs, thereby inhibiting T cell activation in vitro and in vivo.[18] Alefacept has been shown to be efficacious in a limited number of patients with psoriatic arthritis (PsA), a partly debilitating disease that may affect small and large joints and the spine.[19]

However, therapeutic antibodies are huge protein molecules and nonhuman in origin. These often elicit significant side effects attributed to their immunogenicity. They are also susceptible to enzymatic degradation. To circumvent these problems, one approach is to design short peptides or small molecular mimics that will bind to critical areas in target proteins and, like antibodies, will interfere with their activity. In our previous work we have shown that peptides designed from the β-turn region of CD2 could modulate CD2−CD58 interactions.[20,21] The peptides reported in our previous studies were from continuous epitopes of CD2 protein. The crystal structure of CD2 indicated that the interaction surface of CD2 with CD58 has two β-strand structures (F and C strands) with charged residues (Figure 1). The β-strands (Figure 2) consist of eight to

* To whom correspondence should be addressed. Phone: (318) 342-1993. Fax: (318) 342-1737. E-mail: jois@ulm.edu.
[†] National University of Singapore.
[§] University of Louisiana Monroe.
[#] Present address: National Cancer Centre, 11 Hospital Drive, Singapore 169610.

[a] Abbreviations: AET, 2-aminoethylisothiouronium hydrobromide; BCECF-AM, bis-carboxyethylcarboxyfluorescein, acetoxymethyl; BSA, bovine serum albumin; CD, cluster of differentiation; DIPEA, *N*,*N*′-diisopropylethylamine; DMSO, dimethyl sulfoxide; FBS, fetal bovine serum; FITC, fluorescein isothiocynate; fs, femtosecond; HATU, 2-(7-aza-1*H*-benzotriazole-1-yl)-1,1,3,3-tetramethyluronium hexafluorophosphate; hCD2, human cluster of differentiation 2; hCD58, human cluster of differentiation 58; MD, molecular dynamics; MEM-α, minimum essential medium-α; MTT, 3-(4,5-dimethylthiazol-2-yl)-2,5-diphenyltetrazolium bromide; MTT assay, mitochondrial dehydrogenase activity assay; PAL resin, 5-(4-aminomethyl-3,5-dimethoxyphenoxy)valeryl resin; Pen, β, β-dimethylcysteine; ps, picosecond; rmsd, root-mean-squared deviation; TFA, trifluoroacetic acid. Single letter abbreviations are used for amino acids.

10.1021/jm0700868 CCC: $37.00
Published on Web 07/21/2007

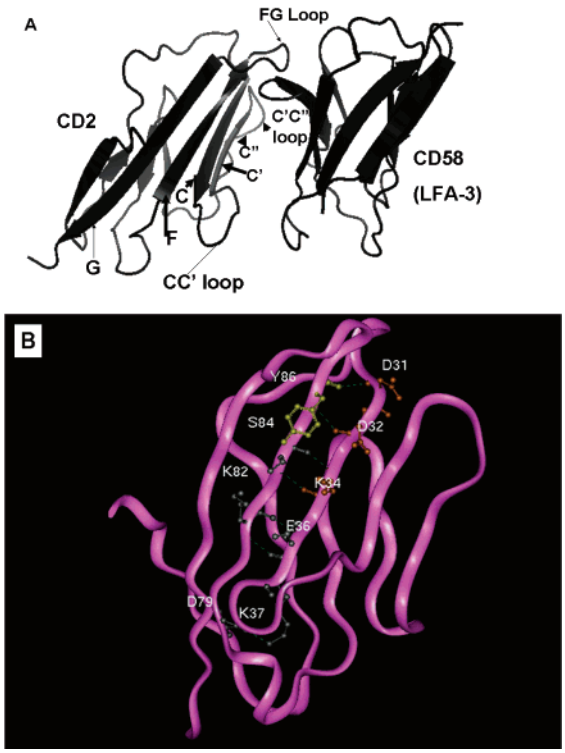

Figure 1. (A**)** Ribbon diagram of crystal structure of hCD2−hCD58 (LFA-3) complex showing different strands of β-sheet. The proposed energetic hot spot and its surroundings in the hCD2−hCD58 interface is shown. (B) CD2 ribbon with the indication of intrastrand hydrogen bonding between C and F strands. Residues from CD2 that are important in the interaction of CD2−CD58 are shown in color. The residues labeled in white font mark the residues in β-strands. For clarity, only important side chains are shown. The broken lines represent hydrogen bonds.

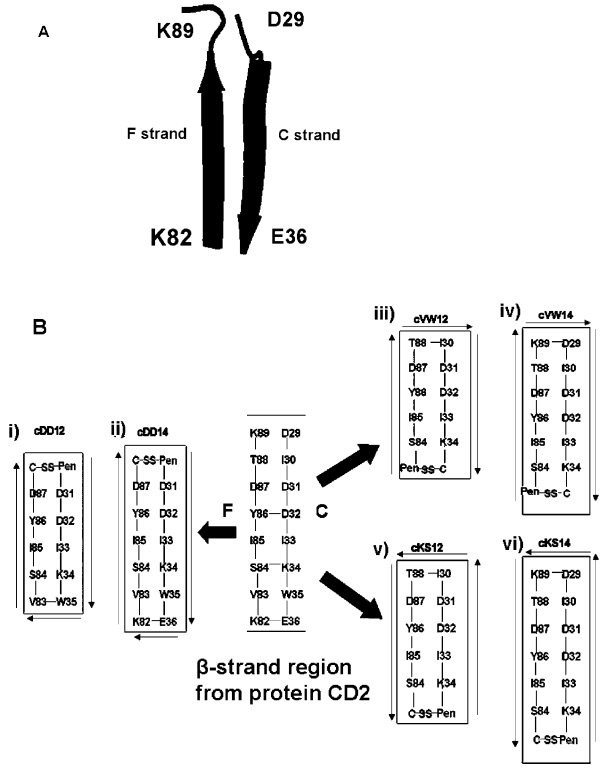

Figure 2. Design of peptides: (A) F and C β strands from CD2 crystal structure; (B) peptides from the discontinuous epitopes of the CD2 protein. The residues in this region are important in binding to CD58. Note that in the cyclic peptides, the two strands are joined by peptide bond or disulfide bond (i−vi). Thin arrows indicate the direction (from N to C terminal) of the peptide sequence.

nine amino acid residues.[8,22,23] Here, our study was undertaken to design small peptides from CD2 that are from discontinuous epitopes to modulate CD2−CD58 interaction and to evaluate their cell adhesion inhibitory activity. These are a new series of peptides from the β-strand regions F and C of CD2 and are designed by conjugating the discontinuous sequences from CD2. Our results indicated that the conjugate peptides designed were able to inhibit E-rosette formation between the Jurkat cell and sheep red-blood cells (SRBC) and to inhibit adhesion between the Jurkat cell and Caco-2 cells.

Results

Preliminary Evaluation of the Structures of the Peptides by Modeling. Peptide epitopes in the native protein acquire a particular 3D structure to interact with other proteins. However, when the amino acid sequence of these epitopes is used for the design of peptides for biological activity, their 3D structures may not be the same as in the native protein. The β-strand peptides designed from CD2 were evaluated using molecular modeling methods to correlate their structure−activity relationship. The crystal structure of CD2 indicated that the interaction surface of CD2 with CD58 has two β-strand structures (F and C strands) with charged residues. The β-strands consist of eight to nine amino acid residues. Close examination of the CD2 crystal structure indicated that the F and C strands are discontinuous in sequence (residues 29−36 and 82−89) but are spatially close and form antiparallel β-sheets (Figure 1) that are 5 Å apart. We hypothesized that conjugation (covalent linking) of these two discontinuous epitopes in small peptide analogues could be useful in modulating CD2−CD58 interaction. Two series of conjugate peptides were designed, one with linear sequences (lDD12, lDD14, lKS12, lKS14) and the other stabilized by the disulfide bridge at the C and N termini to retain the β-sheet conformation.

During conjugation of the peptide sequences, different possible orientations between the two strands and different linking points were considered. The length of the β-strands was varied by changing the number of amino acids in the peptide structure. For example, the peptide lDD12 was designed by choosing six amino acids from the C strand (I30 to W35) and the F strand (V83 to T88). (Throughout the manuscript, single-letter codes for amino acids are used.) The peptide lDD14 was designed by choosing seven amino acids from the C strand (I30 to E36) and the F strand (K82−T88). lDD14 has two additional amino acids compared to lDD12. The two strands were linked by a peptide bond. The cyclic versions of these peptides were designed with a disulfide bond by introducing a Pen residue at the N terminal and a Cys residue at the C terminal of the peptide by replacing the terminal residues. The two strands were connected by a peptide bond on one side and a disulfide bond on the other side. The cyclic peptide cDD14 has a larger ring size than cDD12 (parts i and ii of Figure 2B). The designed peptides are shown in Table 1 and Figure 2B. In each of these peptides the effectiveness of preserving the molecular structure by different types of linking was evaluated by molecular modeling. The four cyclic peptides (cDD12, cDD14, cVW12, and cVW14) were constructed using InsightII software (Accelrys Inc., San Diego, CA), and 10 ps molecular dynamics simulation was carried out to investigate the different possible conformations the peptide could acquire. As shown by preliminary MD calculations, most structures displayed a stable conformation

Table 1. Peptides Designed from the β-Sheet Region of Human CD2 Protein That Forms the Interface of CD2−CD58 Complex in the Crystal Structure[a]

code	sequence[b]
lDD12	I_{30}-D-D-I-K-W_{35}-V_{83}-S-I-Y-D-T_{88}
cDD12	cyclo(1, 12)-Pen-D_{31}-D-I-K-$W_{35-}V_{83-}$S-I-Y-D_{87}-C-OH
lDD14	I_{30}-D-D-I-K-W-E_{36}-K_{82}-V-S-I-Y-D-T_{88}
cDD14	cyclo(1, 14)-Pen-D_{31}-D-I-K-W-E_{36}-K_{82}-V-S-I-Y-D_{87}-C-OH
cVW12[c]	cyclo(1,12)-Pen-S_{84}-I-Y-D-T_{88}-I_{30}-D-D-I-K_{34}-C-OH
cVW14[c]	cyclo(1,14)-Pen-S_{84}-I-Y-D-T-K_{89}-D_{29}-I-D-D-I-K_{34}-C-OH
lKS12	W_{35}-K-I-D-D-I_{30}-T_{88}-D-Y-I-S-V_{83}
cKS12	cyclo(1, 12)-Pen-K_{34}-I-D-D-I_{30}-T_{88-}D-Y-I-S_{84}-C-OH
lKS14	W_{35}-K-I-D-D-I-D_{29}-K_{89}-T-D-Y-I-S_{84}-V_{83}
cKS14	cyclo(1, 14)-Pen-K_{34}-I-D-D-I-D_{29}-K_{89}-T-D-Y-I-S_{84}-C-OH

[a] Refer to Figure 2B for covalent structure of the peptide. [b] The sequence number (subscript) refers to the sequence number in human CD2 protein. Note that all the peptides are derived from the same region; however, the chain direction during conjugation is different. Pen refers to L-penicillamine (L-β,β-dimethylcysteine). [c] Peptides cVW12 and cVW14 were designed and not synthesized.

with a β-strand structure except peptide cVW14. Peptide cVW14 exhibited a flexible structure indicated by the significant difference between the average conformation and the one with minimum energy conformation (Figure 3). It showed a loop conformation instead of a β-strand conformation. The peptide cDD12, which has clockwise linkage between the strands, exhibited β-hairpin conformation. A comparison of the overall structure of the MD derived structure with the structure of a similar sequence fragment in the CD2 crystal structure was carried out. The backbone rmsd between the peptide cVW12 and the structure of the same sequence region in the native protein was 1.89 Å. Peptides cDD12 and cDD14 showed an rmsd of 2.9 and 2.0 Å with the similar fragments in the CD2 crystal structure, respectively (Figure 4). The peptide cVW14 showed a maximum rmsd of 3.33 Å with its native crystal structure. This was very clear from the flexible nature of the cVW14 structure. Thus, molecular modeling studies suggested that cyclic peptides designed from β-strand regions of CD2−CD58 may acquire the same conformation as in the native protein and hence act as good scaffolds for inhibition of CD2−CD58 interaction.

To test the above hypothesis that peptides designed from discontinuous epitopes act as inhibitors of cell−cell adhesion interaction, two model cyclic peptides (cDD14 and cDD12), as well as the linear version of the same peptides without the residues Cys and Pen, were synthesized (Table 1). Since cVW14 showed flexible structure, its reverse sequence peptide cKS14 and its 12 amino acid analogue cKS12 were designed (parts v and vi of Figure 2B). Their linear analogues were also synthesized and investigated for inhibitory activity.

Inhibition of CD2−CD58 Interaction by the Model Peptides. The biological activity of the peptides was evaluated by two inhibition assays. The first method, E-rosetting, was carried out to test the biological activity of peptides.[20,24] E-rosetting is the most widely used method to identify T cells showing CD2−CD58 interaction. Sheep red blood cells express sheep CD58 protein, while Jurkat leukemic T cells express CD2 protein on their surfaces (confirmed by a flow cytometry assay; data not shown). The binding of Jurkat cells to sheep red blood cells due to CD2 and CD58 interaction results in the formation of E-rosettes. The ability of each of the designed CD2 peptides to inhibit CD2−CD58 interaction was evaluated by inhibition of E-rosette formation between Jurkat cells and sheep red blood cells.

Preincubation of sheep red blood cells with T cells with human CD2 derived peptides, but not with a control peptide, resulted in a concentration-dependent inhibition of E-rosette formation (Figure 5). It was observed that all cyclic peptides in this series exhibited 10−20% higher inhibitory activities than the linear peptides. This validates our hypothesis that the cyclization would help short peptides maintain secondary structure as observed in a similar sequence from the CD2 protein crystal structure.

In the series peptides that were derived from clockwise linkage, the linear peptide lDD12 exhibited higher inhibitory activities than the linear peptide lDD14 (about 5% higher at the highest dosage tested). The cyclic version of these peptides, cyclic peptide cDD12, exhibited about 30% activity, and cDD14 exhibited 40% inhibition activity at 200 μM in the E-rosetting assay.

However, in the series of peptides that were generated from anticlockwise linkage, the same trend was found in both linear and cyclic peptides. The linear peptide with 12 amino acids, lKS12, showed higher inhibition activity (35%) than 14 amino acid residue peptide lKS14 (15%). Among the cyclic peptides, the smaller cyclic ring size (peptide cKS12, 46%) showed higher inhibitory activity than the larger cyclic ring size (peptide cKS14, 25%). In addition, the peptide cKS12 was potent (exhibiting about 45% activity at 200 μM in the E-rosetting assay) compared to the peptide cDD14 in inhibiting the cell−cell interaction, indicating that the effect of reversing the sequence of peptide (of cWV12) may change the conformation of the peptide resulting in a conformation that mimics the native structure of the peptide epitope in the CD2 protein crystal structure. As a positive control, antibody to CD58 was used. The antibody showed 100% inhibition at 5 μM concentration or less.

As a second method, inhibition of adhesion between Caco-2 cells and Jurkat cells was used to evaluate the biological activity of the designed peptides.[20,25] Caco-2 cells express human CD58, while Jurkat cells express human CD2 protein; thus, the inhibitory activity observed between Caco-2 cells and Jurkat cells provides evidence that the peptides designed from CD2 can inhibit the heterotypic cell adhesion by the hCD2−hCD58 pathway. By use of fluorescently labeled Jurkat cells, the inhibitory activities of designed CD2 peptides were measured and fluorescence changes were observed with and without peptide addition. This heterotypic adhesion assay is much more sensitive than E-rosetting because of the measurement of fluorescence.[25] The activities of the peptides from CD2 in the heterotypic cell adhesion assay are shown in Figure 6 along with a control peptide. Linear peptides lDD12 and lDD14 exhibited 25% and 30% inhibition activity, respectively. The cyclic peptide cDD14 showed 50% activity at 90 μM, while cKS12 was the most potent among these peptides, showing 60% inhibitory activity at 90 μM in this assay. The trends in the inhibitory activity of peptides were similar to those obtained with the E-rosetting assay.

Statistical analysis of the data using SPSS software indicated that all the peptides showed significant difference with negative control in both assays ($p < 0.05$). All the cyclic peptides showed significant enhanced activity compared to their linear counterparts at 200 μM in the E-rosetting assay. For the lymphocyte epithelial assay, similar results were obtained except for lDD12 and cDD12. Linear and cyclic peptides lDD12 and cDD12 did not show significant difference in inhibition activity at 90 μM in the lymphocyte-epithelial adhesion assay. Positive control CD58 antibody showed nearly 100% inhibition at 5 μM concentration or less. Hence, statistical comparison was not made between the antibody and the peptide described above.

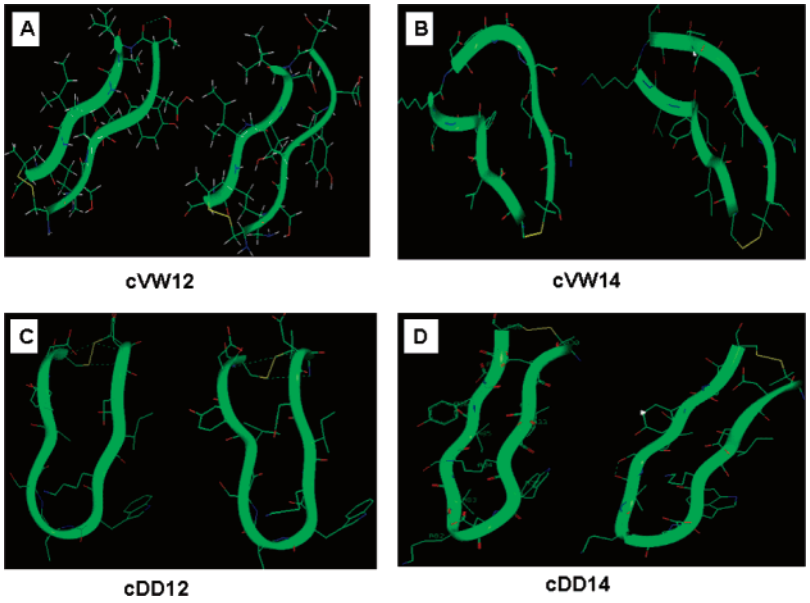

Figure 3. Average (left) and minimum energy (right) conformations of designed CD2 peptides after molecular dynamics simulation in vacuum and energy minimization.

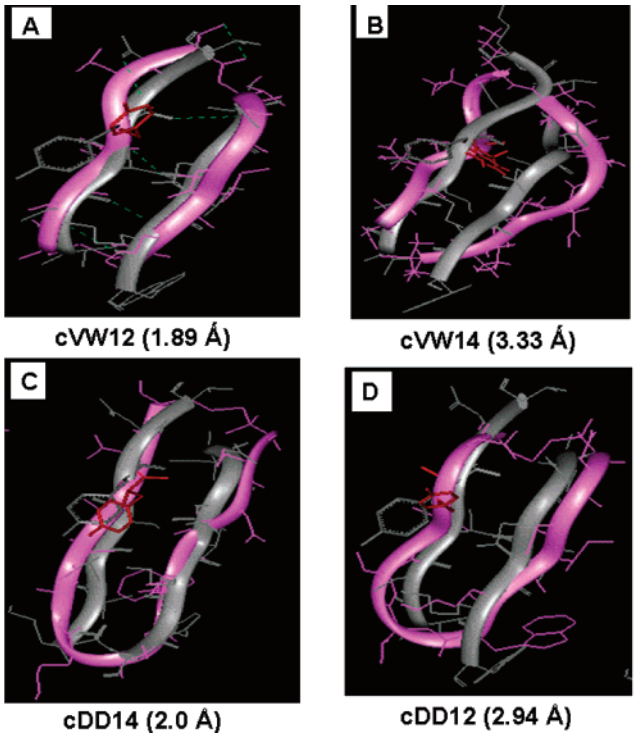

Figure 4. Comparison of the average conformations of designed CD2 peptides after molecular dynamics simulation (purple) with the similar peptide sequence in the crystal structure of hCD2 protein (gray). The numbers in the parentheses give the rms deviations of the backbone atoms (in Å) between the two structures.

Cell Viability Assay. The MTT assay, an index of cell viability and cell growth, is based on the ability of viable cells, not dead cells, to reduce MTT from a yellow water-soluble dye to a dark-blue insoluble formazan product by mitochondrial enzymes associated with metabolic activity.[26] The assay has been widely used in cell proliferation assays, cytotoxicity analyses, and apoptosis screening. To examine the toxicity of the designed peptides, the ability of the peptides to inhibit the growth of human Caco-2 cells and Jurkat cells was assessed in this assay. The results showed that the Caco-2 monolayers or Jurkat cells incubated with the highest dose of peptides for fixed

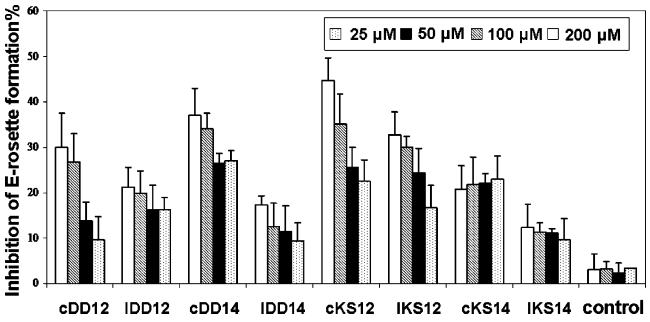

Figure 5. Inhibition of E-rosette formation by synthetic peptides derived from CD2 protein. Peptides were added to AET-treated sheep red blood cells (expressing CD58 protein) first, and then an equal amount of Jurkat cells (expressing CD2 protein) was added later. Cells with five or more SRBCs bound were counted as rosettes. Values are % inhibition of peptide-treated cells and expressed as the mean of three independent experiments.

periods, which were used in the lymphocyte-epithelial adhesion assay, did not display any significant inhibition of the cell viabilities (Figure 7). Therefore, the peptides used in this study were not toxic to the cells, indicating that the mechanisms of the two cell-based adhesion assays may be due to the blocking of CD2−CD58 interaction by these peptides.

Peptides from CD2 Do Not Interfere with ICAM-1/LFA-1 Adhesion. Besides the CD2−CD58 interaction for cell adhesion, β2 integrin LFA-1 and its ligand ICAM-1 (the principal ligand ICAM-1) contribute to the cell adhesion mechanism for immunological synapse formation. These interactions stabilize the interaction between T cells and APCs and provide costimulatory signals.[5,6] Caco-2 cells express ICAM-1 protein (data not shown). We presume that peptides from CD2 inhibit cell adhesion by inhibiting CD2−CD58 interaction and not LFA-1-ICAM-1 mediated adhesion. To help ascertain this mechanism, we performed the Jurkat cell immobilized ICAM-1 adhesion assay in which the cell adhesion is mediated by LFA-1/ICAM-1 interaction. As shown in Figure 8, the Jurkat immobilized ICAM-1 adhesion was significantly inhibited by the CD54 monoclonal antibody (mAb) compared to the control (blank). Cyclic peptides designed from CD2, namely, cDD14 and cKS12, did not inhibit ICAM-1-LFA-1 mediated adhesion.

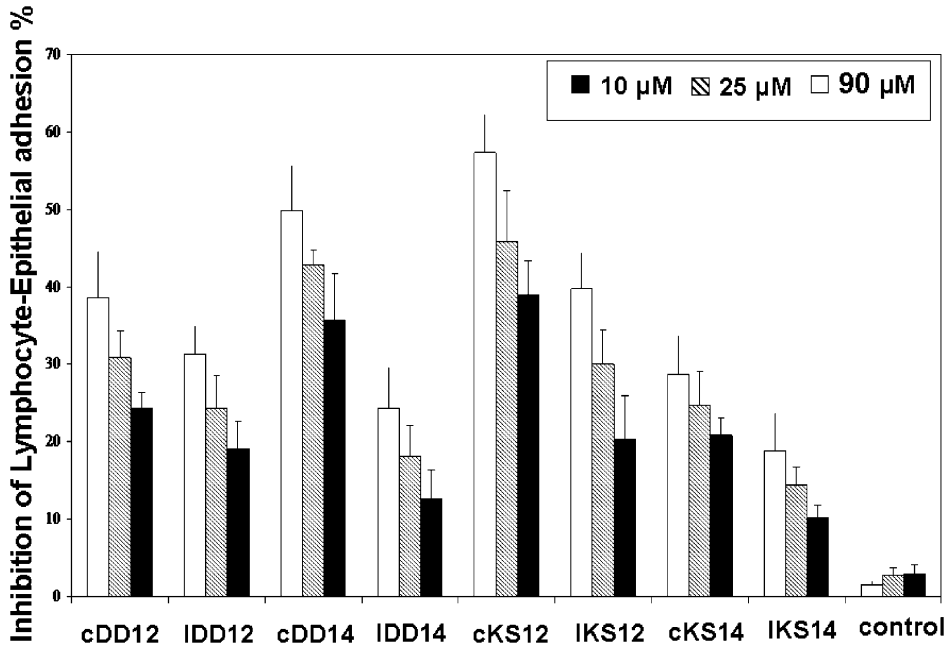

Figure 6. Inhibition of lymphocyte-epithelial adhesion by synthetic peptides derived from CD2 protein. Peptides were added to the confluent Caco-2 monolayer, and then the BCECF labeled Jurkat cells were added to the mixture. After incubation for 45 min at 37 °C, nonadherent Jurkat cells were removed by washing with PBS and the monolayer associated Jurkat cells were lysed with Triton X-100 solution. Soluble lysates are transferred to 96-well plates for reading in a microplate fluorescence analyzer. Values are shown as the % inhibition of peptide-treated cells and expressed as the mean of three independent experiments.

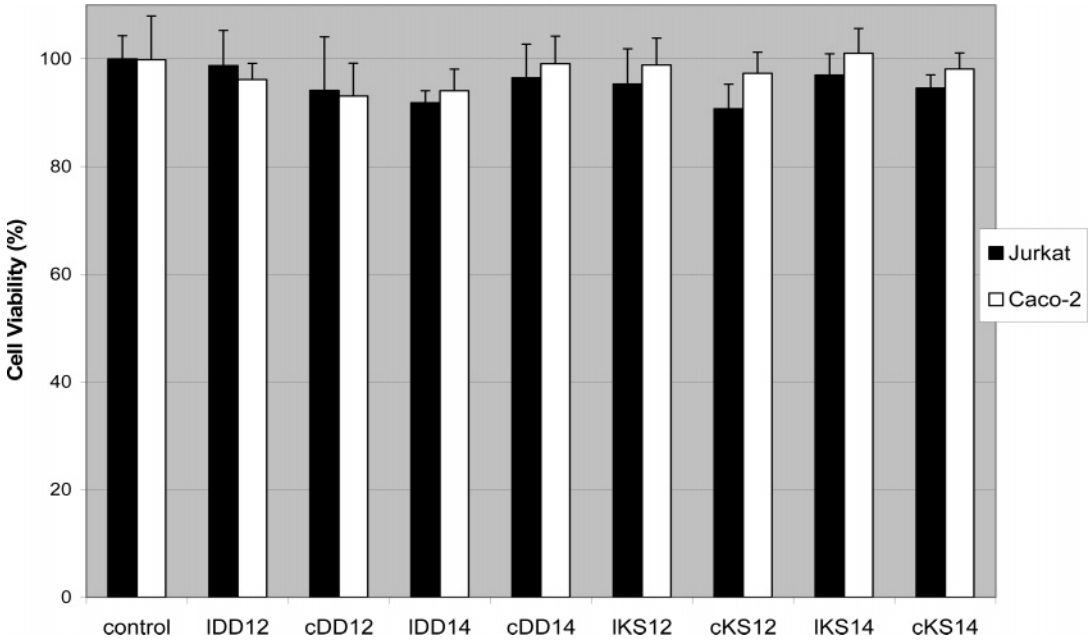

Figure 7. Cell viabilities of Caco-2 monolayers and Jurkat cells treated with synthetic peptides. MTT assay was applied to examine the cytotoxicity of peptides to the Caco-2 cells and Jurkat cells during the lymphocyte-epithelial adhesion assay. All samples were assayed in four independent assays, and the mean for each experiment was calculated.

Circular Dichroism Studies. The circular dichroism spectra of the peptides were recorded in water. The linear peptides lDD12, lDD14, lKS12, and lKS14 (Figure 9) showed a negative band below 200 nm, which suggests the possibility of an open or unordered conformation. The cyclic versions of these peptides (cDD12, cDD14, cKS12, cKS14) each exhibited a negative band around 202−204 nm, indicating the possibility of a type I β-turn conformation (Figure 9).[27,28] The cyclic peptide cDD14 exhibits a negative band at 203 nm and a negative shoulder around 200 nm, suggesting the possibility of a β-strand structure.

Free Molecular Dynamics Simulations of the Model Peptide. Among the peptides studied, peptide cKS12 showed nearly 60% inhibition activity at 90 μM in the lymphocyte-epithelial inhibition assay. To understand the stability of peptide conformation and to correlate the conformation with biological activity, the internal mobility of the model peptide was studied using molecular dynamics simulations. MD studies were carried out on cKS12 model peptide for 200 ps in a water cell. An 8 Å water layer was used during the simulation, and the first 40 ps of the simulation time was excluded for structural analysis.

The mobility of backbone atoms was analyzed during the course of simulation for evaluating the flexibility of the peptides. The backbone torsion angles (φ, ψ) in the two loops (residues 5−8 and 9−12) showed that the peptides did not exhibit large

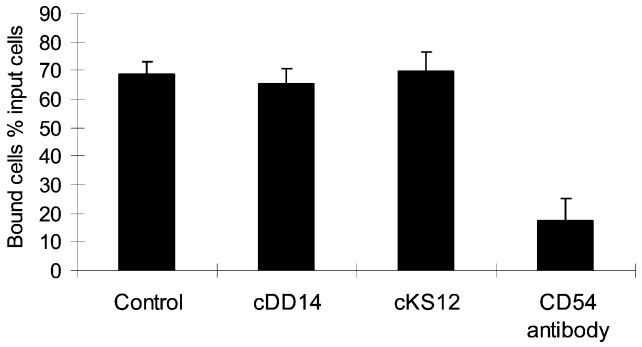

Figure 8. Effect of CD2 peptides on ICAM-1-LFA-1 adhesion. Inhibition of Jurkat cells binding to rhICAM-1 coated on the plates is shown in the figure. The ICAM-1 antibody shows inhibition of Jurkat cells to the ICAM-1 coated plate, whereas peptides from CD2 do not show inhibition.

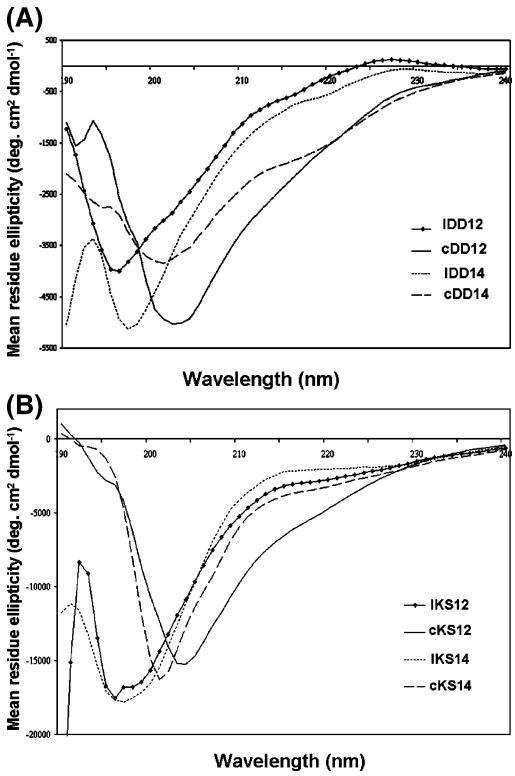

Figure 9. Circular dichroism spectra of (A) lDD12, cDD12, lDD14, and cDD14 and of (B) lKS12, cKS12, lKS14, and cKS14 at pH 7 at 250 μM in water. The legend for different peptides is shown in the figure.

variation from the mean structure or the structure from restrained MD. This was also pronounced for the region corresponding to the β-strand (residues 2−5). Inspection of the Ramachandran plots of the MD trajectory of Φ, ψ values of residues revealed that the conformation (Supporting Information) of the peptide did not change significantly during dynamics.

Discussion

Design of Peptides. As previously noted, the crystal structure of the CD2−CD58 complex indicated that the interaction surface of CD2 with CD58 has two β-strand structures (strands F and C) with charged residues.[8,22,23] The β-strands span eight to nine amino acid residues. These F and C strands are discontinuous in sequence (residues 29−36 and 82−89) but spatially close and form an antiparallel β-sheet (Figures 1B and 2) in which strands are placed apart at 5 Å distance. The residues in these strands have been shown to be important in binding of the CD2 to CD58 protein using mutagenesis studies. Most of the energetics for interactions between the two proteins come from the salt bridges and hydrogen bonds. Ten salt bridges and five hydrogen bonds were found in the crystal structure of the CD2−CD58 complex at the interface.[8] The only hydrophobic contact, from the CD2 side, involves the packing of the aromatic ring of hCD2 Y86 with the aliphatic portion of hCD58 K34. Point mutation studies suggested that in hCD2, the Y86 to A86 mutation (F strand) resulted in a significant loss of binding of CD2 to CD58 (more than 1000-fold), while Y86 to F86 mutation in the same region did not affect the binding. The ϵ-amino group of K34 of CD58 is involved in hydrogen bond formation to D32 of CD2, which helps K34 maintain itself in an extended conformation, thereby ensuring the formation of the small hydrophobic core. This region is identified as the energetic hot spot of the CD2−CD58 interaction.[8] The aromatic rings of Y86 in CD2 and F46 in CD58 create a small but critical hydrophobic core in the CD2−CD58 interface, which is important to the cation−π interaction between the CD2 Y86 aromatic ring and the positively charged ϵ-amino group of CD58 K34. Thus, we proposed that in our peptide design if we retain the C strand with D31, D32, and K34 residues that are close to the hydrophobic region (CD2 and CD58 both have K34 residue) and retain the F strand with "hot spot" Y86, the peptide will mimic the native structure of the protein.

On the basis of the results mentioned above and our previous studies,[20,21] we proposed that a cyclized β-hairpin peptide assembling the two strands (residues 30−36 and 82−88) would be a suitable model for mimicking the CD2 interface with CD58. Stabilization and linkage of the two strands were achieved by the disulfide bridge at the C and N termini. From a survey of β-sheets from a set of 928 nonredundant protein structures,[29] the mean $C^\beta-C^\beta$ distances between hydrogen-bonded and non-hydrogen-bonded pairs of residues in adjacent strands were 4.82 $\pm$ 0.58 and 5.37 $\pm$ 0.56 Å, respectively, while the average $C^\beta-C^\beta$ distance in disulfide-bonded cysteines was 3.84 Å. Therefore, the C^β atoms of opposing residues on antiparallel strands are normally too far apart for disulfide bond formation to effectively reproduce the conformation of the β-strand structure. Nonetheless, disulfide cross-links are sometimes found between cysteines in the non-hydrogen-bonding register in β-sheets.[30,31] Thus, we chose to introduce a cyclic constraint between the C and F strands without modifying the CD2 bioactive conformation and minimum peptide main chain length by varying the number of amino acids in each strand. For the conjugation of the C and F strands, several parameters were considered: (i) residues that are important for CD58 binding, (ii) minimum number of amino acids required for activity, (iii) a change of the backbone orientation by reversal of the sequence, (iv) cyclization by disulfide bond and peptide bond at the two ends of β-strands F and C, and (v) variation in the ring size of the cyclic structure. Introduction of disulfide bonds generated two types of structures: (a) peptides that have a disulfide bond near D87 and D31 and (b) peptides that have a disulfide bond near S84 and K34. The disulfide bridge was generated by introducing penicillamine (Pen) at the N terminal and Cys at the C terminal (Figure 2B). Peptide cDD12 consists of important residues D31, D32 K34, and Y86 and has 12 amino acid residues (part i of Figure 2B). The two strands were joined by a peptide bond at W35−V83 and by a disulfide bond near the D31, D87 end with Pen at the N terminal. Since the N terminal starts at residue D31 and the C terminal is at D87, it is considered as clockwise cyclization. To evaluate the effect of cyclic ring size on the

conformation of the peptide and the biological activity, a larger cyclic ring size with 14 amino acids, cDD14, was designed (part ii of Figure 2B). To examine in which type of linkage and cyclization the peptides would keep the antiparallel β-sheet conformation of native-like protein, two more cyclic 12- or 14-mer peptides were designed by introducing disulfide bonds near the K34 and S84 terminals of the C and F strands (cVW12 and cVW14). To change the backbone orientation of the peptides, the sequences of the peptides were reversed by introducing Pen at K34 (N terminal) and Cys at S84 (C terminal), generating the peptides cKS12 and cKS14. Since these peptide sequences were reversed (compared to the other peptide described above), the peptides cKS12 and cKS14 were considered as anticlockwise cyclization (parts v and vi of Figure 2B). Corresponding linear peptides (lDD12, lDD14, lKS12, and lKS14) were designed to compare the activity of linear and cyclic peptides. Molecular dynamics studies suggested that larger ring size peptide cVW14 conformation did not resemble the native structure of the CD2 epitope. Thus, peptides cVW12 and cVW14 were not synthesized for evaluating biological activity.

Here in our study, we utilized the pharmacophore information (hot spot Y86 and other important residues D31, D32, and K34) and three-dimensional structure information (antiparallel β-sheets) from CD2 C and F strands in the binding of CD2 to CD58. In addition, the distance between the two strands is around 5 Å, which is about the distance of a two amino acid residue linkage suitable for disulfide bond formation. Our concept is entirely conformation-based with the hypothesis that a peptide with incorporation of important residues and cyclization of the peptide by linking the peptide backbone in one terminal by peptide bond and a disulfide bridge in the other terminal would mimic the native CD2 interface that interacts with CD58.

Biological Activity. The inhibitory activities of peptides designed to modulate/block CD2−CD58 interaction were studied by E-rosetting and the lymphocyte-epithelial adhesion (Figures 5 and 6) assays. It was observed that all cyclic peptides in this series exhibited 20−30% higher inhibitory activity than did linear peptides in both assays. Peptide cKS12 showed nearly 60% inhibition activity at 90 μM in the lymphocyte-epithelial adhesion assay. We have described linear single strand peptides from C, C′, C″, and F strands (peptides DS, SE, and IK) in our earlier publication.[21] Peptides cKS12 and cDD14 are derived from the conjugation of DS and IK sequences. DS and IK peptides showed low inhibitory activity (<30% and <20%, respectively). However, conjugation of these peptides resulted in cDD14 and cKS12 enhanced inhibitory activity (60%). The enhanced activity of these peptides could be due to the stable β-strand secondary structure of the peptide after conjugation of linear peptides.

Statistical analysis suggested that cyclic peptides showed enhanced activity compared to linear peptides and all the peptides showed a significant ($p < 0.05$) difference in activity compared to the control peptide. Circular dichroism studies clearly showed that linear peptides displayed random structure in solution while cyclic peptides displayed β-turn structure.[27,28] Consistent with the preliminary molecular modeling results, the cDD14 peptide exhibited higher inhibitory activities than the smaller sized cyclic peptide cDD12. The circular dichroism studies did not show significant difference in the secondary structures (both are β-turn conformations).

However, in the series of peptides that were generated from anticlockwise linkage, both linear and cyclic peptides cKS12 and lKS12 with 12 amino acids were found to be more active than the larger (ring) size peptides (peptide cKS14 and lKS14). The circular dichroism spectra of these peptides suggested the existence of a stable secondary structure in the smaller ring size peptides, especially in the cyclic peptide cKS12. In addition, peptide cKS12 was more potent compared to peptide cDD14 in inhibiting the CD2−CD58 interaction, indicating that the effect of inversing the sequence of the peptide (of cWV12) may change the conformation of the peptide to the one similar to native conformation in the crystal structure of CD2 protein.

In conclusion, we have designed peptides with 12 and 14 amino acid residues from the discontinuous epitopes of CD2 protein. The peptides were designed to mimic C and F strands of CD2 protein. To stabilize the peptides and to retain the native conformation, peptides were cyclized by a disulfide bond and peptide bond at the conjugation points of the two strands. Different possible conjugations of the two strands (the C and F strands) were considered during the design. The cell adhesion inhibitory activity of the peptides using the E-rosetting assay and lymphocyte-epithelial adhesion assay indicated that the designed peptides inhibit the cell−cell adhesion interaction presumably by inhibiting CD2−CD58 interaction. Peptides with smaller cyclic ring size showed higher inhibitory activity compared to larger ring size cyclic structures. Peptides derived from conjugation of the C and F strands of the CD2 protein were more potent in cell-adhesion inhibition compared to the peptides that were designed from single strands of C or F from our previous studies.[20,21] Thus, the introduction of conformational constraints on the peptide backbone through disulfide bridges in the terminals of the peptides from C and F strand regions imparts changes in potency with inhibition of CD2−CD58 interaction. Furthermore, peptides derived from CD2 did not show any inhibitory activity for ICAM-1-LFA-1 cell adhesion, indicating that peptides may be specific for interfering with CD2−CD58 mediated cell adhesion.

Materials and Methods

Peptides. The linear peptides (Table 1) were designed and synthesized, and the cyclic peptides were purchased from Multiple Peptide Systems (San Diego, CA). The pure products were analyzed by HPLC and electrospray mass spectrometry (ESI-MS). The HPLC chromatogram showed that the purities of peptides were more than 90%, and ESI-MS showed the correct molecular ion for the peptides. Linear peptides lDD12, lDD14, lKS12, and lKS14 and the control peptide were synthesized using an automatic solid-phase peptide synthesizer (Pioneer, Perspective Biosystem) using Fmoc chemistry. The Fmoc-protected amino acids were obtained from Novabiochem. All the solvents used in the Pioneer protein synthesizer were obtained from Applied Biosystems (Foster, CA).

Synthesis of Linear Peptides. PAL resin (5-(4-*N*-Fmoc-aminomethyl-3,5-dimethoxyphenoxy)valeryl) was used as solid support for the linear peptides.[32,33] First, the Fmoc protecting group on the resin was removed by treatment with 20% piperidine/DMF. The N^{α}-Fmoc-amino acids were preactivated by mixing with the coupling reagent HATU/DIPEA (1: 1). The activated amino acid was then added to the resin and mixed at room temperature. Cycles of deprotection of Fmoc and coupling with the subsequent amino acids were repeated until the desired peptide-bound resin was completed. The resin was washed manually with DMF, DCM, and methanol successively to remove the excess solvents and dried in vacuo over KOH overnight before cleavage and deprotection. The dried peptidyl-resin was mixed with the cleavage cocktail (90% TFA, 5% thioanisole, and 5% 1,2-ethanedithiol, 5 mL per gram of resin) and precipitated with cold ether. For maximum recovery, the ether−peptide mixture was kept at −20 °C overnight. Then the precipitated material was collected by centrifugation and washed three times with cold ether to remove any residual scavengers. After evaporation of the ether, the peptide was dissolved in water with a few drops of acetic acid and lyophilized.

The lyophilized peptide was dissolved in water/acetonitrile. Peptide was purified by preparative HPLC (waters 600 HPLC system) on a reversed-phase C18 column (Inertsil, 10 mm × 250 mm, 5 μm, 300 Å) with a linear gradient of solvent A (0.1% TFA/H_2O) and solvent B (0.1% TFA/acetonitrile). The peptide was detected by UV at $\lambda = 215$ and 280 nm. The purity of each peptide was verified by analytical HPLC (Shimadzu LC-10AT VP) using a reversed-phase C18 column (Lichrosorb RP18, 4.6 mm × 200 mm, 10 μm) with the same solvent system as in the preparative HPLC. The molecular weight of the peptides was confirmed by using ESI-MS (Finnigon MAT). The HPLC chromatogram showed that the purity of the peptides was more than 90%, while ESI-MS showed the correct molecular ion for the peptide.

Cell Lines. The Jurkat T-leukemia and the human colon adenocarcinoma cell lines (Caco-2) were obtained from the American Type Culture Collection (Rockville, MD). Jurkat cells were maintained in suspension in RPMI1640 medium supplemented with 10% heat-inactivated fetal bovine serum (FBS) and 100 mg/L penicillin/streptomycin. Caco-2 cells were maintained in minimum essential medium-α containing 10% FBS, 1% nonessential amino acids, 1 mM Na pyruvate, 1% L-glutamine, and 100 mg/L penicillin /streptomycin. Caco-2 cells were used between passages 50 and 60. Sheep blood in Alsever's solution was purchased from TCS Biosciences Ltd., Singapore.

E-Rosetting. Sheep red blood cells (SRBCs) were isolated by centrifuging sheep blood in Alsever's solution at 200*g* for 5 min. SRBCs were washed three times with PBS and incubated with four volumes of AET solution at 37 °C for 15 min. The cells were washed three times in PBS and resuspended in RPMI-1640 containing 20% FBS to give a 10% suspension. For use, the cell suspension was diluted 1:20 (0.5%) with medium. Serial dilutions of peptides in PBS were added to 0.2 mL of 0.5% AET-treated SRBCs and incubated at 37 °C for 30 min. After that, 0.2 mL of the Jurkat cell suspension (2×10^6/mL) was added to the mixture and incubated for another 15 min. The cells were pelleted by centrifugation (200*g*, 5 min, 4 °C) and then incubated at 4 °C for 1 h. The cell pellet was gently resuspended, and the E-rosettes were counted with a hemocytometer.[24] Cells with five or more SRBCs bound were counted as rosettes. At least 200 cells were counted to determine the percentage of E-rosette cells. The inhibitory activity was calculated by the following equation,

$$\text{inhibition (\%)} = \frac{\text{non-RFC}_{\text{treated with peptide}} - \text{non-RFC}_{\text{blank}}}{\text{RFC}_{\text{blank}}} \times 100$$

where RFC is E-rosette forming cells.

Lymphocyte-Epithelial Adhesion Assay. Caco-2 cells were used between passages 50 and 60 and were plated onto 48-well plate at approximately 2×10^4 cells/well. When the cells reached confluency, the monolayers were washed once with MEM-α. Jurkat cells were labeled the same day as the adhesion assay by loading with 2 μM fluorescent dye BCECF at 37 °C for 1 h. Peptide dissolved in MEM-α was added at various concentrations to Caco-2 cell monolayers. After incubation at 37 °C for 30 min, the labeled Jurkat cells (1×10^6 cells/well) were added onto the monolayers. After incubation at 37 °C for 45 min, nonadherent Jurkat cells were removed by washing three times with PBS, and the monolayer-associated Jurkat cells were lysed with 2% Triton X-100 in 0.2 M NaOH. Soluble lysates were transferred to 96-well plates for reading with a microplate fluorescence analyzer.[34] Data are presented as relative fluorescence or percent inhibition as described previously.[25] Relative fluorescence (FL) was found by reading the values of fluorescence intensity corrected for the reading of background (cell monolayers only).

Statistical analysis of the results from the cell adhesion assay was carried out using the Mann−Whitney *U* test ($n = 4$) utilizing SPSS software. Peptides were grouped into two categories for the analysis based on their sequence origin (group 1 contained lDD12, lDD14, cDD12, and cDD14; group 2 contained lKS12, lKS14, cKS12, and cKS14). Within each group the peptides are linear and cyclic. The *p* values were compared for analysis.

Cell Viability Assay. Peptides that exhibited effects on Jurkat Caco-2 adherence were tested by MTT assay[26] to determine if their effects were due to its toxicity. A final concentration of 180 μM peptide was added to Jurkat or Caco-2 cells for 1 or 2 h, which is the maximum time of exposure of Caco-2/Jurkat cells during the adherence assay. The cell viabilities were validated by incubating with 5 mg/mL MTT at 37 °C for 3 h. The MTT-labeled cells were lysed by DMSO, and the absorbance was measured with a microplate reader at a wavelength of 570 nm.

Circular Dichroism Measurement. Circular dichroism experiments were carried out at room temperature on a Jasco J-810 spectropolarimeter flushed with nitrogen. Spectra were collected from 240 to 190 nm using 1 mm path length of cylindrical quartz cell. Each spectrum was the average of three scans taken at a scan rate of 50 nm/min with a spectral bandwidth of 1 nm. The concentration of peptides was varied from 0.15 to 2.5 mM. For the final representation, the baseline was subtracted from the spectrum.

Jurkat-Immobilized ICAM-1 Adhesion. Phorbol ester, 12-myristate 13-acetate (PMA), bovine serum albumin (BSA), and penicillin G sodium salt were purchased from Sigma-Aldrich Co. (St. Louis, MO). Hank's balanced salt solution (HBSS), streptomycin sulfate, magnesium sulfate, and calcium chloride dihydrate were from Sigma Chemical Co. (St. Louis, MO). Bis-carboxyethylcarboxyfluorescein, acetoxymethyl (BCECF, AM) was obtained from Molecular Probes (Eugene, OR), and Triton X-100 was purchased from Bio-Rad Laboratories (Hercules, CA). RPMI 1640 medium was purchased from Gibco Invitrogen Corporation (Grand Island, NY), and fetal bovine serum (FBS) was provided by Hyclone Laboratories, Inc. (Logan, UT). Mouse anti-human CD54 (ICAM-1) domain D1 monoclonal antibody (clone 15.2) was purchased from Ancell Corporation (Bayport, MN). Recombinant human intercellular adhesion molecule-1 (rhICAM-1) was purchased from R & D Systems (Minneapolis, MN).

Effect of Peptides on LFA-1/ICAM-1 Adhesion. Since LFA-1/ICAM-1 adhesion is cation-dependent, HBSS/1%BSA buffer (HBSS containing 1%BSA, 2 mM Mg^{2+}, and 2 mM Ca^{2+}, adjusting to pH 7.4) was used to ensure effective binding[35] of the two proteins. The 96-well plates were coated and left overnight at 4 °C with 50 μL/well rhICAM-1 (5 μg/mL in PBS). Plates were washed three times and then blocked with HBSS/1%BSA for 1 h at room temperature. Peptides (200 μM), CD54 mAb (5 μg/mL), or HBSS/1%BSA alone (blank) were added and incubated for 30 min. Jurkat cells were labeled with BCECF as described under the heterotypic adhesion assay, and 1.5×10^5 cells resuspended in HBSS/1%BSA were added to each well in the presence of PMA (50 ng/mL). The tumor-promoting agent (PMA) can induce and enhance LFA-1 mediated adhesion by activation of protein kinase C (PKC), which enhances the affinity of LFA-1 for ligands.[36]

The plates were incubated at 37 °C for 1 h, and nonadherent cells were removed by gently washing the plates three times with HBSS/1%BSA. The bound cells were lysed with 2% Triton X-100 in 0.1 M NaOH and incubated at 37 °C for 1 h. For the total fluorescence of input cells, labeled Jurkat cell suspension was centrifuged at 2000 rpm for 5 min, and the cell pellet was lysed with 2% Triton X-100 in 0.1 M NaOH at 37 °C for 1 h. The fluorescence of aliquots of 1.5×10^5 cells/well represented the total input cells, and the proportion of bound cells was expressed as the fluorescence percentage of input cells.

Molecular Dynamics (MD) Simulations. Molecular dynamics simulations were carried out using InsightII/Discover software (Accelrys, Inc., San Diego, CA),[37] version 2000, on a Silicon Graphics computer. Consistent valence force field (cvff) was used. Two methods were used: the first method to model the peptide structure and the second method to evaluate the detailed conformation of peptide cKS12 using MD simulations for an extended period of time.

Procedure A. The structures of model peptides cVW12, cVW14, cDD12, and cDD14 were simulated by first constructing the peptide structures based on CD2 protein fragments. The two strands of the β-sheet were cyclized by peptide bond and disulfide bond. The resulting structure with optimized disulfide bond was subjected to

MD simulation in vacuum for 10 ps with a time step of 1 fs. Structures were saved every 100 fs for further analysis. The first 3 ps of the simulations was not used for the analysis. From a plot of time vs energy of the remaining 7 ps MD trajectory, an average structure was chosen as the representative conformation. The average structure was further energy-minimized using the steepest descents method and conjugate gradient method until the rms derivative was 0.3 kcal/mol Å. The rms deviation of the backbone atoms were compared between the average structure and the energy-minimized structure. An rmsd comparison was also made between the average structure and the three-dimensional structure of the similar fragment in the CD2 protein.

Procedure B. The peptide cKS12 was modeled as described in procedure A. The conformation stability of the peptide cKS12 was analyzed for its stability by extended-time MD simulation. The average structure obtained from MD simulation was soaked in a layer of water with a thickness of 8 Å from the center of the peptide, which is large enough to cover the whole peptide. The MD simulation was carried out without any constraints for 200 ps with pre-equilibration for 10 ps. Trajectory was analyzed by plotting time on the *x*-axis and different variables along the *y*-axis. The first 40 ps of the simulations was not considered during the analysis. To monitor the stability of conformation of the peptide, pseudotorsion angles were considered. Selected parameters presented are τ "pseudotorsion angles" ($C\alpha_i-C\alpha_{i+1}-C\alpha_{i+2}-C\alpha_{i+3}$) defined by the Cα atoms of residues 2−5, 5−8, and 9−12.

NMR Spectroscopy. The sample for the NMR spectrum of the cyclic peptides was prepared by dissolving 1−3 mg of the peptide in 0.6 mL of 90% H_2O/10% D_2O at the pH with the best dispersion. For pH titration experiments, the pH of the solution was varied by the addition of DCl or NaOD (pH was not corrected for isotopic effects). The one- and two-dimensional NMR experiments were performed and processed on 300, 600, and 700 MHz Bruker DRX spectrometers equipped with a 5 mm probe, at a proton frequency of 300.3414 and 600.1299 MHz, respectively, using the XWIN-NMR, version 1.0, software. Spectra were acquired at 298 and 293 K unless otherwise specified. TOCSY,[38] DQF-COSY,[39] and rotating frame nuclear Overhauser spectroscopy (ROESY)[40] experiments were performed by presaturation of water during relaxation delay in 500 and 700 MHz NMR instruments. NMR spectra were analyzed by SPARKY[41] software. Assignment of the spin system was carried out using TOCSY spectrum for each peptide.

Acknowledgment. We gratefully acknowledge the Super Computer and Visualization Unit and NMR facility at the National University of Singapore, Singapore. This research was funded by Academic Research Grant R-148-000-026-112 from the National University of Singapore, Singapore, and a startup grant from the College of Pharmacy, University of Louisiana at Monroe, LA. The authors thank Dr. Ronald Hill and Ms. Oliver from University of Louisiana at Monroe for their useful suggestions.

Supporting Information Available: ^{1}H NMR, HPLC, MS, and purity data; conformational changes of loops for cKS12 peptide during MD simulation. This material is available free of charge via the Internet at http://pubs.acs.org.

References

(1) Cemerski, S.; Shaw, A. Immune synapse in T-cell activation. *Curr. Opin. Immunol.* **2006**, *18*, 1−7.
(2) Van der Merwe, P. A.; Davis, S. J. Molecular interactions mediating T cell antigen recognition. *Annu. Rev. Immunol.* **2003**, *21*, 659−684.
(3) Grakoui, A.; Bromley, S. K.; Sumen, C.; Davis, M. M.; Shaw, A. S.; Allen, P. M.; Dustin, M. L. The immunological synapse: a molecular machine controlling T cell activation. *Science* **1999**, *285*, 221−227.
(4) Bromley, S. K.; Burack, W. R.; Johnson, K. G.; Somersalo, K.; Sims, T. N.; Sumen, C.; Davis, M. M.; Shaw, A. S.; Allen, P. M.; Dustin, M. L. The immunological synapse. *Annu. Rev. Immunol.* **2001**, *19*, 375−396.
(5) Bierer, B. E.; Burakoff, S. J. T cell adhesion molecules. *FASEB J.* **1998**, *2*, 2584−2590.
(6) Springer, T. A. Adhesion receptors of the immune system. *Nature* **1990**, *346*, 425−434.
(7) Ulbrich, H.; Eriksson, E. E.; Lindbom, L. Leukocyte and endothelial cell adhesion molecules as targets for therapeutic interventions in inflammatory disease. *Trends Pharmacol. Sci.* **2003**, *24*, 640−647.
(8) Kim, M.; Sun, Z. Y.; Byron, O.; Campbell, G.; Wagner, G.; Wang, J.; Reinherz, E. L. Molecular dissection of the CD2−C58 counter-receptor interface identifies CD2 Tyr86 and CD58 Lys34 residues as the functional "hot spot". *J. Mol. Biol.* **2001**, *312*, 711−720.
(9) Davis, S. J.; Ikemizu, S.; Evans, E. J.; Fugger, L.; Bakker, T. L.; van der Merwe, P. A. The nature of molecular recognition by T-cells. *Nat. Immunol.* **2003**, *4*, 217−224.
(10) Davis, S. J.; van der Merwe, P. A. The structure and ligand interactions of CD2: implications for T cell function. *Immunol. Today* **1996**, *17*, 177−187.
(11) Bachmann, M. F.; Barner, M.; Kopf, M. CD2 sets quantitative thresholds in T cell activation. *J. Exp. Med.* **1999**, *190*, 1383−1391.
(12) Hoffmann, J. C.; Herklotz, C.; Zeidler, H.; Bayer, B.; Rosenthal, H.; Westermann, J. Initiation and perpetuation of rat adjuvant arthritis is inhibited by the anti-CD2 monoclonal antibody (mAb) OX34. *Ann. Rheum. Dis.* **1997**, *56*, 716−722.
(13) Sido, B.; Dengler, T. J.; Otto, G. Differential immunosuppressive activity of monoclonal CD2 antibodies on allograft rejection versus specific antibody production. *Eur. J. Immunol.* **1998**, *28*, 1347−1357.
(14) Przepiorka, D.; Phillips, G. L.; Ratanatharathorn, V.; Cottler-Fox, M.; Sehn, L. H.; Antin, J. H.; LeBherz, D.; Awwad, M.; Hope, J.; McClain, J. B. A phase II study of BTI-322, a monoclonal anti-CD2 antibody, for treatment of steroid-resistant acute graft-versus-host disease. *Blood* **1998**, *92*, 4066−4071.
(15) Squifflet, J. P.; Besse, T.; Malaise, J.; Mourad, M.; Delcorde, C.; Hope, J. A.; Pirson, Y. BTI-322 for induction therapy after renal transplantation: a randomized study. *Transplant. Proc.* **1997**, *29*, 317−319.
(16) Besse, T.; Malaise, J.; Mourad, M.; Pirson, Y.; Hope, J.; Awwad, M.; White-Scharf, M.; Squifflet, J. P. Prevention of rejection with BTI-322 after renal transplantation (results at 9 months). *Transplant. Proc.* **1997**, *29*, 2425−2426.
(17) Spitzer, T. R.; McAfee, S. L.; Dey, B. R.; Colby, C.; Hope, J.; Grossberg, H. T. R.; Preffer, F.; Shaffer, J.; Alexander, S. I.; Sachs, D. H.; Sykes, M. Nonmyeloablative haploidentical stem-cell transplantation using anti-CD2 monoclonal antibody (MEDI-507)-based conditioning for refractory hematologic malignancies. *Transplantation* **2003**, *75*, 1748−1751.
(18) Mrowietz, U. Treatment targeted to cell surface epitopes. *Clin. Exp. Dermatol.* **2002**, *27*, 591−596.
(19) Braun, J.; Sieper, J. Role of novel biological therapies in psoriatic arthritis: effects on joints and skin. *BioDrugs* **2003**, *17*, 187−199.
(20) Jining, L.; Makagiansar, I.; Yusuf-Makagiansar, H.; Chow, V. T.; Siahaan, T. J.; Jois, S. D. Design, structure and biological activity of beta-turn peptides of CD2 protein for inhibition of T-cell adhesion. *Eur. J. Biochem.* **2004**, *271*, 2873−2886.
(21) Liu, J.; Ying, J.; Chow, V. T.; Hruby, V. J.; Satyanarayanajois, S. D. Structure−activity studies of peptides from the "hot spot" region of human CD2 protein: development of peptides for immunomodulation. *J. Med. Chem.* **2005**, *48*, 6236−6249.
(22) Wang, J.; Smolyar, A.; Tan, K.; Liu, J.; Kim, M.; Sun, Z. J.; Wagner, G.; Reinherz, E. L. Structure of a heterophilic adhesion complex between the human CD2 and CD58 (LFA-3) counterreceptors. *Cell* **1999**, *97*, 791−803.
(23) Davis, S. J.; Davies, E. A.; Tucknott, M. G.; Jones, E. Y.; van der Merwe, P. A. The role of charged residues mediating low affinity protein−protein recognition at the cell surface by CD2. *Proc. Natl. Acad. Sci. U.S.A.* **1998**, *95*, 5490−5494.
(24) Albert-Wolf, M.; Meuer, S. C.; Wallich, R. Dual function of recombinant human CD58: inhibition of T-cell adhesion and activation via the CD2 pathway. *Int. Immunol.* **1991**, *3*, 1335−1347.
(25) Liu, J.; Chow, V. T.; Jois, S. D. A novel, rapid and sensitive heterotypic cell adhesion assay for CD2-CD58 interaction, and its application for testing inhibitory peptides. *J. Immunol. Methods* **2004**, *291*, 39−49.
(26) Mosmann, T. Rapid colorimetric assay for cellular growth and survival: application to proliferation and cytotoxicity assays. *J. Immunol. Methods* **1983**, *5*, 55−63.
(27) Perczel, A.; Fasman, G. D. Analysis of the circular dichroism spectrum of proteins using the convex constraint algorithm: a practical guide. *Anal. Biochem.* **1992**, *203*, 83−93.
(28) Perczel, A.; Fasman, G. D. Quantitative analysis of cyclic β-turn models. *Protein Sci.* **1992**, *1*, 378−395.
(29) Hutchinson, E. G.; Sessions, R. B.; Thornton, J. M.; Woolfson, D. N. Determinants of strand register in antiparallel beta-sheets of proteins. *Protein Sci.* **1998**, *7*, 2287−2300.

(30) Maynard, A. J.; Sharman, G. J.; Searle, M. S. Origin of beta-hairpin stability in solution: structural and thermodynamic analysis of the folding of a model peptide supports hydrophobic stabilization in water. *J. Am. Chem. Soc*. **1998**, *120*, 1996−2007.
(31) Hutchinson, E. G.; Sessions, R. B.; Thornton, J. M.; Woolfson, D. N. Determinants of strand register in antiparallel beta-sheets of proteins. *Protein Sci.* **1998**, *7*, 2287−2300.
(32) *Handbook of Combinatorial and Solid Phase Organic Chemistry: A Guide to Principles, Products and Protocols*; Advanced Chemtech: Louisville, KY, 1998; pp 329−372.
(33) Lloyd-Williams, P.; Albericio, F.; Giralt, E. *Chemical Approaches to the Synthesis of Peptides and Proteins*; CRC: Boca Raton, FL, 1997; Chapter 2, pp 19−82.
(34) Gines, S.; Marino, M.; Mallol, J.; Canela, E. I.; Morimoto, C.; Callebaut, C.; Hovanessian, A.; Casado, V.; Lluis, C.; Franco, R. Regulation of epithelial and lymphocyte cell adhesion by adenosine deaminase−CD26 interaction. *Biochem. J.* **2002**, *361*, 203−209.
(35) Anderson, M. E.; Siahaan, T. J. Targeting ICAM-1/LFA-1 interaction for controlling autoimmune diseases: designing peptide and small molecule inhibitors. *Peptides* **2003**, *24*, 487−501.
(36) Cherry, L. K.; Weber, K. S.; Klickstein, L. B. A dominant Jurkat T cell mutation that inhibits LFA-1-mediated cell adhesion is associated with increased cell growth. *J. Immunol.* **2001**, *167*, 6171−6179.
(37) *InsightII*; Accelrys, Inc.: San Diego, CA. InsightII is a commercial, licensed molecular modeling software. Obtained from Accelrys, Inc.: http://www.accelrys.com/products/insight/
(38) Bax, A.; Davis, D. G. MLEV-17-based two-dimensional homonuclear magnetization transfer spectroscopy. *J. Magn. Reson.* **1985**, *65*, 355−360.
(39) Rance, M.; Sorensen, O. W.; Bodenhausen, G.; Wagner, G.; Ernst, R. R.; Wüthrich, K. Improved spectral resolution in COSY ^{1}H NMR spectra of protein via double quantum filtering. *Biochem. Biophys. Res. Commun*. **1983**, *117*, 479−485.
(40) Bax, A.; Davis, D. G. Practical aspects of two-dimensional transverse NOE spectroscopy. *J. Magn. Reson*. **1985**, *63*, 207−213.
(41) Goddard, T. D.; Kneller, D. G. *SPARKY3*; University of California: San Francisco, CA; http://www.cgl.ucsf.edu/home/sparky/.

JM0700868